JOURNAL OF FORENSIC SCIENCES

J Forensic Sci, May 2012, Vol. 57, No. 3
doi: 10.1111/j.1556-4029.2012.02056.x
Available online at: onlinelibrary.wiley.com

PAPER

CRIMINALISTICS

Sonia P. Sant,[1] *B.Sc. (Hons.) and Scott I. Fairgrieve,*[1] *Ph.D.*

Exsanguinated Blood Volume Estimation Using Fractal Analysis of Digital Images*

ABSTRACT: The estimation of bloodstain volume using fractal analysis of digital images of passive blood stains is presented. Binary digital photos of bloodstains of known volumes (ranging from 1 to 7 mL), dispersed in a defined area, were subjected to image analysis using FracLac V. 2.0 for ImageJ. The box-counting method was used to generate a fractal dimension for each trial. A positive correlation between the generated fractal number and the volume of blood was found (R^2 = 0.99). Regression equations were produced to estimate the volume of blood in blind trials. An error rate ranging from 78% for 1 mL to 7% for 6 mL demonstrated that as the volume increases so does the accuracy of the volume estimation. This method used in the preliminary study proved that bloodstain patterns may be deconstructed into mathematical parameters, thus removing the subjective element inherent in other methods of volume estimation.

KEYWORDS: forensic science, criminalistics, blood stain pattern analysis, blood volume estimation, fractal analysis

Bloodstain pattern analysis provides investigators with a valuable tool for interpreting the dynamics of a crime scene. This field represents a multidisciplinary approach to crime scene dynamics and integrates the fields of physics, chemistry, biology, rheology, hematology, and mathematics in such a way as to assist in reconstructing the events that yielded observed bloodstain patterns. The interpretation of bloodstain patterns is dependent upon understanding the dynamics of blood as a biological fluid (1–8). The shedding of blood and the formation of stains may occur through blood flowing freely from an open wound, spreading as a pool, through direct transfer via contact, or through the action of being cast-off from the blood source either passively or projected.

As a viscous fluid, blood is a connective tissue consisting of 45% plasma and 55% formed elements including red blood cells, white blood cells, and platelets. The average adult human has 60–66 mL of blood per kg of body weight, with a range of 5.7 L for men and 4.3 L for women (2). Blood is noted to have a characteristic surface tension and density (3). It is now understood that blood has both Newtonian and non-Newtonian characteristics. This behavioral duality can be traced back to the unique composition of blood. Plasma is regarded as being Newtonian in that it forms droplets owing to weak surface tension, whereas the formed elements in the blood are considered to be non-Newtonian and form drops owing to internal cohesion (3).

Bloodstain pattern analysis is based on the tenet that blood will act in a predictable manner when subjected to external forces in accordance with the laws of physics (1). Its behavior is therefore predictable and reproducible, forming the basis of its admissibility in court. Although satisfying court standards, the area of bloodstain pattern analysis is heavily reliant on the expertise of the analyst and that individual's experience in interpreting such evidence at the scene. It is possible that a variety of mechanisms, or a combination thereof, may give rise to similar patterns in complicated, dynamic scenes. Hence, more objective analytical approaches need to be established.

Of the analytical methodologies that are part of bloodstain pattern analysis, there is currently no scientifically accepted or court qualified methodology for the quantification of single-event exsanguinated blood volume from bloodstain evidence at crime scenes. The amount of blood lost by a victim may be vital in the determination of postinjury survival time, the location of severe or lethal injuries, and the likelihood of death when no body is found (1–3).

The estimation of the volume of blood shed has previously relied upon direct and indirect methods of measurement (9,10). The direct measurement studies by Lee examined either lifting dry blood from a nonabsorbent surface and measuring the weight, or by weighing the bloodstained areas of an absorbent material (such as carpet) and subtracting the weight of an unstained area of the same size. Conversion factors were derived in order to provide an estimate of the blood volume (9,10).

Lee also attempted indirect methods whereby a grid is placed over a large bloodstained area and the number of squares covering the stain is counted. The weight of one occupied square and one blank square is measured (as in the case of carpeting). The difference in values provides a unit weight of the blood, and this is then multiplied by the total number of units covering blood. A conversion factor is then used to estimate the volume. A similar process is used for nonporous surfaces; however, the grid is then photographed in place and the bloodstained and unstained areas are then cut out and weighed accordingly (11). The relative proportions of these two values are used as a basis for the estimated volume.

There are many problems inherent with the methods proposed by Lee. However, the foremost of these is that Lee fails to report the statistics and standard error rates for each of these methods. Although there is a broad volumetric estimation for each of these

[1]Department of Forensic Science, Laurentian University, 935 Ramsey Lake Road, Sudbury, ON P3E 2C6, Canada.

*Presented at the 62nd Annual Meeting of the American Academy of Forensic Sciences, February 22–27, 2010, in Seattle, WA.

Received 14 Aug. 2010; and in revised form 3 April 2011; accepted 16 April 2011.

methods, they all lack essential statistical support as required by *Daubert* standards of scientific evidence.

Additionally, these reported methods lack sufficient technical details to make them practical. Likewise, the methods proposed for absorbent substrates assume uniform density of such surfaces. The photographic methods fail to account for any standardization of angle or height. The use of a direct method is destructive and assumes that samples required for estimation were taken as part of the evidence gathering process or that the examiner has direct access to the scene. The use of photographs in indirect methods however makes use of evidence that is a normal part of evidence collection and hence will be readily available for examination.

Consequently, the aim of this paper is to present a novel indirect method for the estimation of exsanguinated blood volume from a single blood-letting event. This new methodology utilizes digital photographs of defined areas that have bloodstains formed from a known volume of blood and distributed over this area by means of passive drops from a syringe under the force of gravity from a fixed height. The bloodstain patterns recorded by the digital photographs were then quantified using fractal analysis of these images.

Fractal Geometry

Lee's methods represent a classical approach to a measurement where a complex shape is approximated by the summation of standard Euclidean shapes. While this method can be used as an estimation, these approximations ignore the very irregularity that classifies a natural pattern. The complex shapes present in bloodstain patterns, as with many other real world objects, do not lend themselves to such simple quantifications as circles, spheres, squares, or cubes. Many natural objects are characterized by a high degree of irregularity and are not amenable to description through strict parameters outlined by simple Euclidean geometry (11).

Benoit Mandelbrot (12) proposed a mathematical means to quantify complex natural structures using a noninteger dimension (13). Fractal, or fractional dimensions, is in evidence throughout nature in the shapes of clouds, mountains, leaves, ferns, fluid flow, and even weather patterns (11,13–16).

The fractal dimension of an object is a measure of its irregularity at all scales. It can be a fractional amount greater than the classical Euclidean dimension of an object. The fractal dimension is a defined mathematical concept related to how fast the estimated measurement of the object increases as the measuring device becomes smaller. As such, a higher fractal dimension means the fractal is more irregular and the estimated measurement increases more rapidly. For example, if one were to measure the fractal coastline of an island, such as Britain, and a "measuring stick" used to do so is 200 miles long, the resulting perimeter is 1600 miles (12). However, if the measuring stick is shortened to 25 miles, the measured perimeter "increases" to 2550 miles. Hence, the British coastline is a fractal object whose fractal dimension is >1. Therefore, a fractal is then an object that has a fractal dimension that is greater than its classic dimension (13).

Mandelbrot (12) further describes fractals as consisting of patterns that recur upon finer and finer magnifications building up shapes of immense complexity. This characteristic is referred to as self-similarity; patterns observed at different magnifications, although not identical, can be described by the same statistics (15,16).

Although fractal objects exist in nature, fractal patterns can also be mathematically generated through an iteration process with the fractal pattern increasing in complexity with each iteration. The Koch curve is a mathematical construct whose Hausdorff fractal dimension can be calculated exactly as 1.26 (12,14). As such, it can be used as a calibration tool.

Mathematical quantification in the form of dimensional analysis is a technique that can be utilized to describe the morphometric complexity of nonlinear, natural fractals. All fractal patterns have properties in common, these are as follows: fractional dimensions, complexity or irregularity at all scales, infinite branching, statistical self-similarity at all scales, and chaotic dynamics (13).

Fractal Analysis and Bloodstain Patterns

The authors theorized that the characterization of bloodstain patterns, with their irregular and complex shapes, is ideally suited to fractal analysis. Such an analysis permits the simplification and quantification of different bloodstains into a single numerical value that defines its shape complexity (17). Only the outer border of a stain pattern is fractal, while the amorphous interior is considered to be Euclidean (17). However, it is the entirety of the stain pattern, comprised of many individual stains, that is being evaluated through fractal analysis in order to derive a unique fractal dimension. The fractal dimension should then be able to capture and account for bloodstain diameter, spine quantity, and impact velocity, thus solving the problem of quantifying naturally complex patterns.

The literature clearly supports the use of fractal geometry to describe other complex shapes and to apply such characterizations to estimate blood volume from bloodstain patterns (11,17–22).

Materials and Methods

Individual passive drops of blood were dispensed using a 30 cc syringe fitted with an 18-gauge, 1.5-inch needle from a standardized height of 40 cm. This height was selected in order to minimize any external environmental variables associated with drop formation and impact velocity. The dispensing of drops was performed by manually depressing the plunger of the syringe in such a way that individual drops formed and subsequently detached themselves from the tip of the needle under the force of gravity. Both the needle and syringe were cleaned or replaced after each completed release of a volume in order to prevent clot formation.

The blood used in this study was sterile sheep's blood obtained from the National Research Council of Canada (Ottawa, Ontario) and was treated with 1% sodium fluoride to act as an anticoagulant and preservative. The blood was refrigerated until needed and gently inverted every 5–6 days to ensure uniformity. The blood was allowed to passively reach room temperature (20°C) prior to use.

The target surface was a sheet of white 24 lb-weight, 117 brightness (on the TAPPI scale), acid-free, printer paper measuring 54 cm by 43.2 cm. The use of printer paper is reported in the literature (6,7). The area of the target was selected for manageability and photographic purposes. The selection of the paper was based on reducing the effects of capillary action inherent in most paper and to reduce crinkling distortion during drying.

The test volumes were purposefully low (1–7 mL) in order to test the level of detection and standard error. The test volumes began at 1 mL and were increased by 1 mL until 7 mL was reached. There were a total of seven trials for each volume.

The drops were deposited in such a way that overlapping stains were minimized. However, as volumes increased, some overlap was inevitable.

Each target was subsequently photographed using a Nikon® D-50 digital camera (Nikon Canada Inc., Mississauga, Ontario,

Canada), on a tripod at a height of 54 cm (camera charged coupled device [CCD] to target distance) under standardized lighting conditions (Fig. 1). The camera was set to manual focus with no flash, on aperture priority, ISO 200, f/11, and recorded as RAW (NEF) images. White balancing was performed using a blank substrate under the standardized lighting conditions. Lighting was provided by two adjustable height, continuous studio lamps with 10.5-inch reflector hoods and were fitted with 60 W bulbs in addition to ambient room fluorescent lighting. The positioning of lights was performed to minimize glare and shadows. The camera's CCD was aligned to be parallel with the substrate using a spirit level, thus addressing concerns with parallax. A translucent white spatter box surrounded the margins of the target to contain radiating spatter. All photographs were taken immediately after the formation of the bloodstain pattern, prior to drying.

Digital Image Processing

All images were copied and converted to a TIFF image from the original RAW (NEF) image. The boundaries of each image were examined and cropped in order to assure that only the defined area of the substrate was considered for the final fractal analysis. The blank substrate photos were treated in the same manner in order to assure that some aspect of the substrate was not contributing to the fractal quantification of the image.

Each image was enhanced by first using the "auto contrast" command and subsequently by using the "replace color" function; selecting the lightest substrate area and adjusting the lightness to 100%, to reduce or eliminate any shadow effects from the lighting. The image was then converted to a gray scale image, and the "burn tool" was used to enhance the boundaries of the blood spatter by increasing the exposure along the borders. Gaps in the spatter, an artifact of reflected light during the exposure, were filled using the pencil tool set at 2 pixels. The resulting image was then converted to a bitmap binary image.

Fractal Image Analysis

Prior to using the chosen software for the fractal quantification of the image, FracLac V. 2.0 for ImageJ (http://imagej.nih.gov/ij/plugins/fraclac/FLHelp/Introduction.htm) (18) needed to be calibrated in order to reliably apply the box-count method. Fractal curves of known dimensions, using binary images of four Koch curves using increasing multiple iterations (4–7), were generated by Fractal Generator, a plugin for ImageJ. These images were then uploaded to FracLac V. 2.0, and the standard box count was applied using a minimum of 2 pixels. In keeping with the literature, the maximum box size was set to 100% of the range of the image (15,16). The number of grid positions overlaid was set at 1. The grid position refers to the location a grid is applied to an image in a box count. The number of occupied boxes will differ depending on where the grid is placed, resulting in different fractal values.

FIG. 1—*Laboratory setup of photographic equipment with standardized lighting (Photo by S. Sant).*

Each binary image of a blood stain pattern was uploaded to FracLac V. 2.0 for ImageJ. Parameters for the standard box count were set to those used for the aforementioned calibration. The "show data for each grid" option was selected, and regression lines were chosen as the graphic to represent these data. The raw data for each grid size were downloaded into MS Excel® (Microsoft Corporation, Redmond, WA). A plot of the –ln (L) versus ln *N* (L), the negative ln of the box size verses the ln of the number of boxes containing occupied pixels, was created. This is the scaling plot of these data, and the fractal dimension is extracted from the slope of the line of best fit. A second graph was created and fitted with two lines of best fit to characterize the dual fractal dimension. A separate scaling plot of each stain pattern was generated in order to obtain the unique fractal dimension. The compiled fractal dimensions were graphed for each volume, and a logarithmic regression analysis was performed using MS Excel® to obtain the volume predictive equations.

A blind trial was conducted to test the validity of the resulting predictive equations for estimated blood volume. Ten different blood volumes, ranging from 1 to 7 mL, unknown to the analyst, were dispensed and analyzed using the above protocol. Unknown volumes were chosen using a random number generator. The fractal dimension was then determined from the slope of the resulting scaling plot. This value was then substituted into the logarithmic regression equation to estimate the unknown volume.

All statistical tests were performed using MS Excel® (Microsoft Corporation, Redmond, WA). The average percent error was calculated for the generated Koch curves. The associated standard error rates and percent deviations were calculated using the known and predicted values for blood volume estimations.

Results

Calibration

The blank substrate yielded a fractal of 0.0. Hence, the background for each of the bloodstain patterns quantified using this technique did not contribute to the fractal quantification of the images. The Koch curves yielded an average fractal value of 1.286; the accepted value for the Koch curve, independent of the number of iterations, is 1.26. Hence, there is a 2.1% error. With such a small error rate, it was decided to continue with the assessment of the binary bloodstain pattern photographs.

Bloodstain Pattern Fractal Dimensions

The production of the bloodstain patterns using the passive distribution method described above resulted in a primary pattern and an accompanying secondary spatter. These two patterns are easily recognizable as they differ in their respective size, shape, and distribution. The primary bloodstains are relatively large with defined scalloped borders. The secondary spatter displays smaller circular

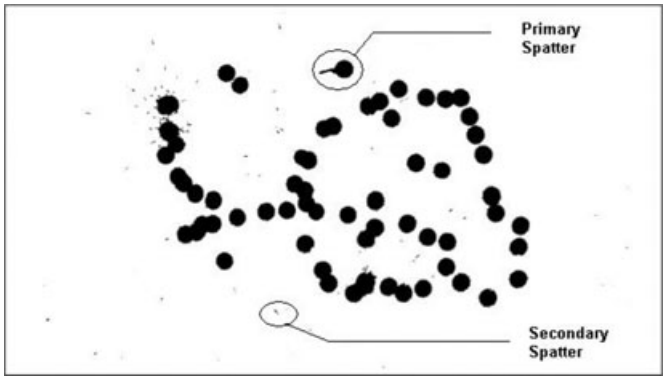

FIG. 2—*Binary image of primary and secondary passively dropped blood.*

bloodstains formed by droplets that have resulted from the force of the impact of the initially dropped blood. Hence, this may also be referred to as satellite spatter (Fig. 2).

The fractal dimension for each replicate volume of blood was calculated by plotting −ln (L) versus ln *N* (L) represented by the slope of the scaling plot (Fig. 3). These data display a power law relationship on a plot of box size versus the number of grid boxes that contain pixels in a box-counting scan, L versus *N* (L). Each bloodstain pattern was characterized by a single fractal dimension that was extracted from the slope of the linear portion of the generated scaling plot (when a natural logarithmic transformation is performed (Fig. 4)). Further analysis shows a fractal dimension duality with primary and secondary patterns characterized by a different fractal dimension (Fig. 5).

A logarithmic regression of the plot of fractal dimension versus volume yielded the following predictive equation (Fig. 6):

$$y = 0.1351 \ln(x) + 14.158 \quad R^2 = 0.84412$$

The equation was then used to predict the volume for each of the samples whose fractal dimension was derived from FracLac. Plotting these values versus the actual sample volume used for each set provided the predictive errors in the calculated value and the range of our error bars for each step volume. This gave the average percent deviation from the known values (Fig. 7). This error range was 77% for 1 mL to 5% for a 7 mL samples.

Using this equation for the blind trials, the error rate ranged from 78% to 7% and was consistently higher for smaller volumes (1 mL) than for larger ones (6 mL) (Table 1 and Fig. 8).

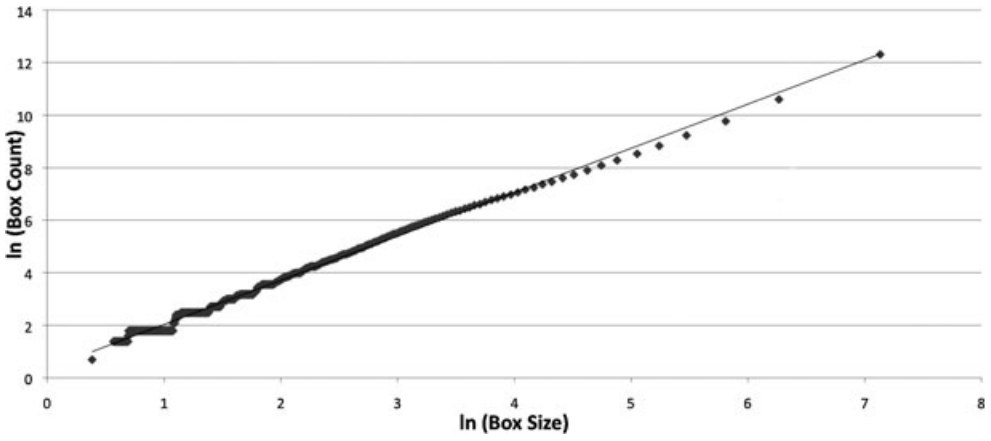

FIG. 3—*Scaling plot from which the fractal dimension is extracted.*

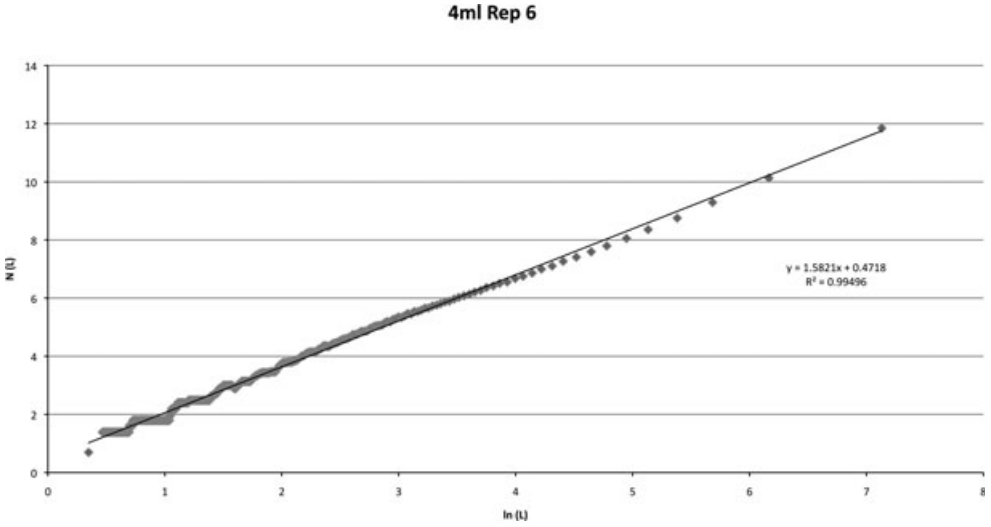

FIG. 4—*Scaling plot of −ln (L) versus ln N (L) using a single slope analysis of the blood stain pattern for 4 mL of blood.*

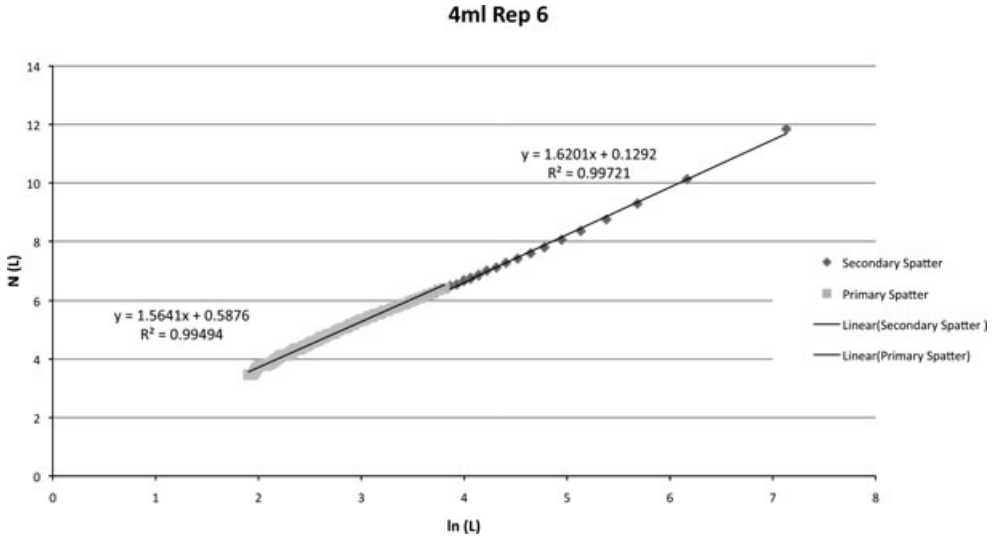

FIG. 5—*Scaling plot of −ln (L) versus ln N (L) using a dual slope analysis characterizing primary and secondary blood stain patterns for 4 mL of blood.*

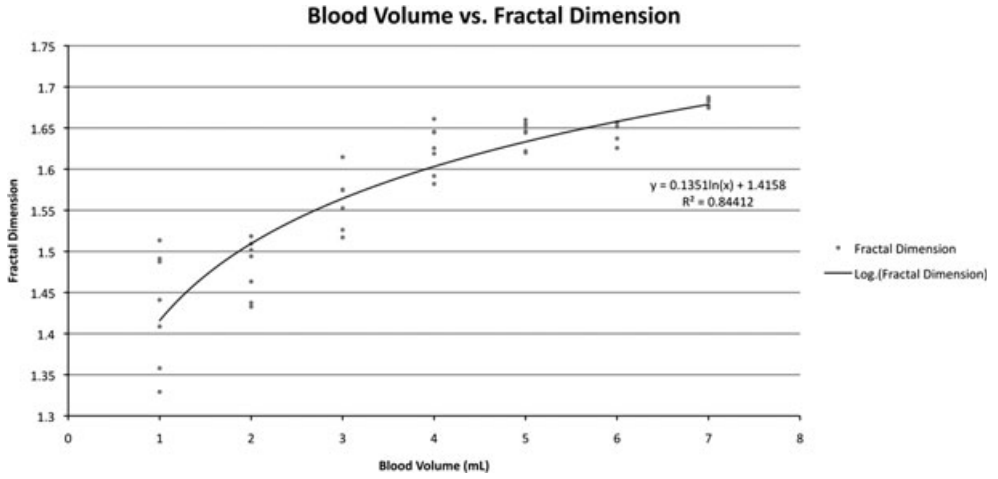

FIG. 6—*Logarithmic regression predictive graph for fractal blood volume.*

Discussion

The overall form of bloodstains from passively dropped blood produce roughly circular stains with scalloped edges. The formation of these edges is owing to the pressure of the fluid at the moment of impact; the strength of the surface tension is overcome at certain points along the drop's margin (6,7). In mid-air, blood is held together in drop form by internal cohesion, which is a much stronger force than surface tension. This acts to limit the degree of scalloping. In some instances, the formation of a scalloped border may also result in a bead of blood being separated from the rest of the blood drop at the time of impact. This is the means by which a secondary spatter is generated in these stains. Hence, these stains, as with those encountered at crime scenes, may be composed of primary and secondary spatter. The use of fractal image analysis as a means of quantifying bloodstains is ideal to detect the dual nature of these stains.

All of the experiments conducted in this study used a constant release height. Additionally, using a syringe as the source of the blood drop acted to keep the relative volume of each drop as close to one another as possible. This was performed as part of the experimental design to control as many factors as possible. Yet, it must be noted that in actual cases, the nature of the surface on which a drop forms and the height at which it falls may be quite variable (17). The drop may form at the end of a knife held by an assailant or the end of a finger as a bleeding victim's blood accumulates at the end of a finger. In combination with the speed, a droplet is projected from the formation surface, droplets of varying volumes are possible.

Bevel and Gardner (17) report drops that result from gravitational forces as having diameters as large as 5 or 5.5 mm with volumes of *c.* 60 μL. This volume is considered to be the upper limit for a stable blood droplet (17).

It is because of this variation in volume that this study used the entire volume of blood dispensed onto each target as the basis for generating the predictive equations. Regardless of the controlled height for dispensing blood, there was still variation in the resulting stain diameter owing to the varying rates of pressure on the syringe plunger and the accumulation of blood elements at the tip of the syringe.

The dispensing height of the blood drop is not the central issue in this study. It is the total volume of the blood that has been dispensed onto a target surface that is of concern. Hence, the method of analysis is not just another way of measuring the diameters of

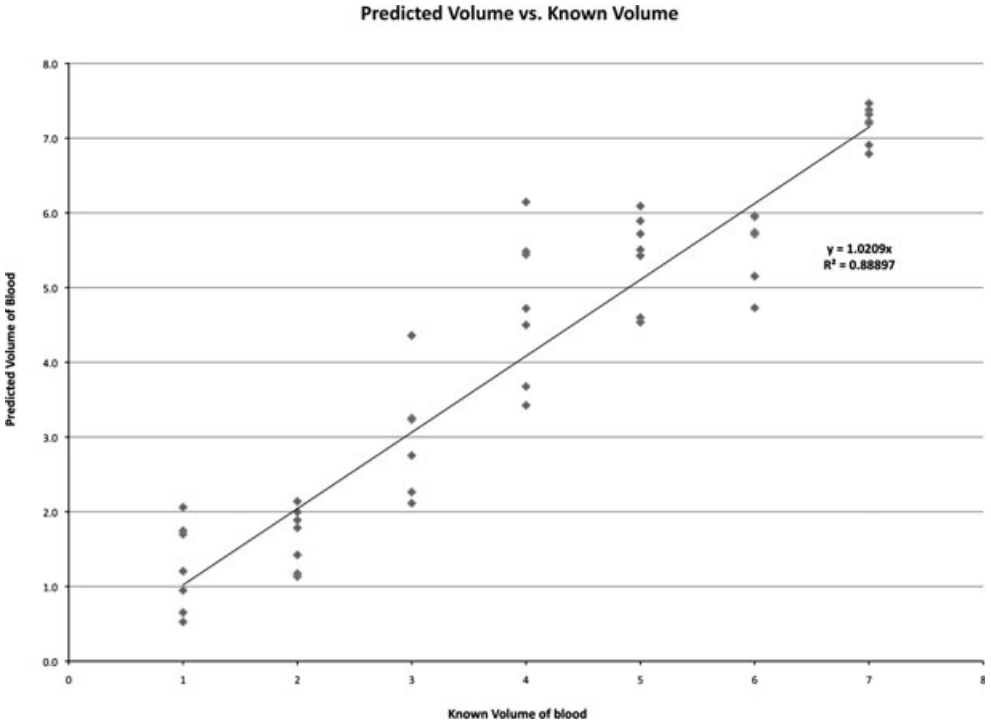

FIG. 7—*Predicted volume of blood versus known blood volumes with associated error rates.*

each stain formed from an individual drop. It is a method for quantifying a volume of blood that covers a substrate given a particular target size as defined by the boundaries of the digital photograph.

The blind trial was to test whether a volume of blood deposited onto the surface of the target could be predicted based on the resulting fractal analysis of the image. The blind trial is the first step in verifying the premise of using fractal analysis for the quantification of blood stains over a given area on a target surface resulting from a specific volume of blood. This is not to suggest that this technique is ready for use in the field at this time. It is recognized that further scenarios of blood shedding events, with other factors being varied, need to be explored with this technique that will enhance its use in practical applications.

By testing this method of quantification on a blank substrate, and yielding a fractal value of 0.0, our chosen substrate did not contribute any background noise. Hence, it was the bloodstains that were being quantified and not artifacts of the substrate. Had any background noise been detected, it would have to be filtered out in order to arrive at an accurate fractal dimension characterizing only the fractal stain and not the background material. Background noise may become more of an issue as the study is expanded to include more substrates with an irregular surface and color.

Further confirmation of this methodology was verified through the quantification of fractal curves of known and accepted Hausdorff dimension (17,18). Koch curves of fractal dimension, 1.26, were generated using four to seven iterations, as recommended in the literature (12,15,16). The calculated fractal dimension was within 2.1% of the expected value. Accordingly, the error can be attributed to the pixilation and resolution of the generated image (20,23).

A power law relationship is observed when the box size is plotted against the number of grid boxes that contain pixels in a box-counting scan. This relationship can be described by the general equation $y = e^{mx} + b$. This relationship is reported in the literature for fractal patterns (15,16). A logarithmic manipulation is needed to yield a linear relationship and subsequent extraction of the fractal dimension.

A scaling plot was generated by a natural logarithm manipulation by graphing –ln (L) versus ln N (L), −ln of the box size versus ln of the number of boxes that contain occupied pixels. The fractal dimension was extracted from the slope of the linear portion of the generated scaling plot. The 49 plots generated for each trial yielded a unique fractal dimension.

Extraction of the fractal dimension from the scaling plots demonstrated that blood passive stains can be characterized by a unique fractal dimension that accounts for shape complexity. A more detailed analysis revealed that the results may be better characterized by two slopes and hence two fractal dimensions. This dual fractal nature has been recognized in the literature (15,16) as the result of two different mechanisms of generation. Examination of generated stain patterns shows two different types of spatter. Primary spatter is displayed by the larger passive droplets, created from the first contact of the liquid with the substrate and secondary

TABLE 1—*A comparison of actual and calculated blood volumes from the blind trial.*

Unknown No.	Calculated Volume	Actual Blind Test Volume	Estimated Fractal Dimension	Absolute Error	Percent Error
1	0.70	1	1.3683	−0.30	30
2	7.79	7	1.6932	0.79	11
3	2.41	3	1.5351	−0.58	19
4	3.76	4	1.5949	−0.24	6
5	3.97	5	1.6021	−1.02	21
6	2.37	3	1. 5329	−0.62	21
7	5.59	6	1.6485	−0.40	7
8	0.21	1	1.2108	−0.78	78
9	1.60	2	1.4794	−0.40	20
10	3.27	4	1.5859	−0.73	18

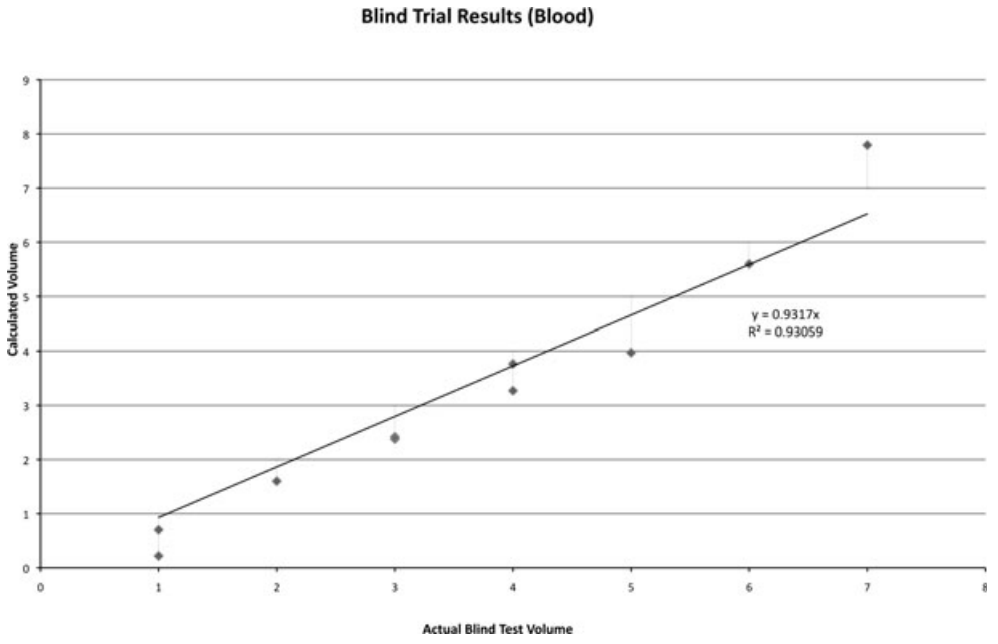

FIG. 8—*Calculated blood volume versus actual blind test blood volume with associated error rates.*

spatter can be seen as the smaller radiating stains that occur as a result of the initial impact.

Bloodstain patterns result from multiple contributing mechanisms producing multiple fractal dimensions, each on a different scale, over which these mechanisms act (20,24). Fractal patterns are the visual outcome of a chaotic system; therefore, the more contributing forces involved in the generation of the stain, the more fractal its borders will be. All the competing forces and factors, which give rise to the irregular nature of the shape of the stain, are accounted for in the fractal dimension value.

The ability of the analysis to detect the secondary spatter speaks to the sensitivity of this method. Secondary spatter occupies a minute portion of the overall examined image. Although this method can detect minute secondary contributions, the analysis used a single slope best-fit method to extract the fractal dimension. This is justified by the extremely high regression coefficient, all within the range of 0.99. Single slope analysis is appropriate within the volume constraints of 1–7 mL as used in this study. At higher volumes, the contribution from secondary mechanisms may increase to the point where dual slope analysis is warranted.

All results for the prediction of blood volumes were acceptable within the errors calculated for each volume sample. The larger errors associated with the smaller volumes are understandable because the lower volume patterns are considerably less fractal in nature than the higher volumes. This is observed both visually through the observations of the stain pattern and in the literature (15,16). As the applied volume increased and the patterns became more fractal, the percent error decreased to 5%. These patterns of observations were mirrored in the results of the blind trial.

The regression yielded a logarithmic function that was theoretically predicted from the power law. The fractal dimension approaches two asymptotically. Mathematical theory suggests that as the fractal dimension of a two-dimensional natural object increases, it will do so as a limit, approaching, but never reaching, 2.0. This suggests that a mathematical exploration of the upper limit of the predictive equation is warranted. The equation has a lower limit of applicability at 1.0 mL. Although the calibration using the blank substrate calculated a fractal dimension of 0.0, this is not accounted for in the equation. Volumes between 0.0 and 1.0 mL should not be estimated using this equation. These limits do not pose a practical problem in the lower limit, but is of importance in the upper limit concerning larger volume blood loss.

Unknown volumes were accurately estimated with percent errors mirroring the trend previously observed with bloodstain samples. The percent errors were greater for lower volumes than for higher volumes as previously discussed. The absolute error, calculated as the difference in milliliters between the calculated volume and the actual test volume, was consistently <1 mL and is therefore insignificant at larger volumes.

Conclusions

Chaos theory and fractal geometry can be applied in a systematic method to assist in the quantitative analysis and modeling of bloodstains by a unique geometric Hausdorff fractal dimension using the box-count method. Results can be used to generate logarithmic regression predictive equations for blood as supported by blind trial evaluation. Error rates and other statistical parameters may be calculated to estimate the reliability of the results.

This technique is limited by the factors that will affect or hinder the determination of the fractal dimension. This includes variability in underlying dispersion mechanisms not accounted for in the generation of the standard graph. The predictive equations should only be applied under tested parameters within the set volume range for passive drop stains on the specified substrate. There is potential for the prediction of larger volumes at lower error rates if the observed patterns are proved to be valid through further testing. The theoretical upper limit as calculated for a fractal dimension approaches 2.0, and, by extrapolation, the point at which the shape becomes Euclidean, is *c.* 75.0 mL.

This study has established a relationship between the fractal dimension and blood volume. Having established the existence of this relationship, the next logical step is an exploration of the factors that may influence the parameters of the predictive equation. Increased blood volume and expansion to different substrates are imperative. A matrix may be developed to include these variables.

This method was developed for passive stains, and hence, work should be carried out to expand its applicability to stains generated by other means.

Fractal theory suggests that this method is independent of scaling and that the slope of the line from which fractal dimension is extracted should remain constant. The effect of scaling should be a shift up or down of the intercept constant in the equation without a change in the slope. This suggests that the fractal dimension would remain constant at different scales. We have explored and verified this for negative scaling by decreasing the box size from 100% of the range of image to 2 pixels. A further exploration of "zooming out" or increasing the scale and the application of larger initial box sizes should be explored.

The applicability to photographs of other resolutions should also be explored. Although it is reported in the literature that pixilation and resolution pose limitations to the determination of the fractal dimension, the extent of their influence remains unclear.

The results of this study reveal that stain patterns are characterized by a fractal dimension duality related to primary and secondary spatter. This study used a single line of best fit for the slope. Further investigation is warranted using a two-slope analysis to determine the significance of the competing generating forces.

Acknowledgments

The authors wish to express their appreciation to Gary Clark from the Department of Physics at Laurentian University for providing guidance on the fractal quantification of digital images. This paper is dedicated to the memory of Dr. Brian H. Kaye, Department of Physics, Laurentian University. His work inspired us to take a walk through fractal dimensions. Finally, we wish to thank the two anonymous reviewers of this manuscript for their helpful suggestions.

References

1. Eckert WG, James SH. Interpretation of bloodstain evidence at crime scenes, 2nd edn. Boca Raton, FL: CRC Press, 1998.
2. James SH. Scientific and legal applications of bloodstain pattern analysis of bloodstain pattern interpretation. Boca Raton, FL: CRC Press, 1999.
3. Wonder AY. Bloodstain pattern evidence: objective approaches and case applications. New York, NY: Elsevier, 2007.
4. Pizzola PA, Roth S, De Forest PR. Blood droplet dynamics I. J Forensic Sci 1986;31(1):36–49.
5. Pizzola PA, Roth S, De Forest PR. Blood droplet dynamics II. J Forensic Sci 1986;31(1):50–65.
6. Hulse-Smith L, Mehdizadeh NZ, Sanjeev C. Deducing impact velocity and droplet size from circular bloodstains. J Forensic Sci 2005;50(1):1–10.
7. Hulse-Smith L, Illes M. A blind trial evaluation of a crime scene methodology for deducing impact velocity and droplet size from circular bloodstains. J Forensic Sci 2007;52(1):65–74.
8. Knock C, Davison M. Predicting the position of the source of blood stains for angled impacts. J Forensic Sci 2007;52(5):1044–9.
9. Lee HC. Estimation of original volume of bloodstains. IAI News 1986;7:11–2.
10. Lee HC. Correction on estimation of original volume of bloodstains. IAI News 1986;9:4.
11. Kaandorp JA. Fractal modeling: growth and form in biology. Berlin, Germany: Springer-Verlag, 1994.
12. Mandelbrot BB. The fractal geometry of nature. New York, NY: W.H. Freeman and Company, 1983.
13. Gleick J. Chaos: making a new science. New York, NY: Penguin Books, 1987.
14. Wegner T, Tyler B. Fractal creations, 2nd edn. Corte Madera, CA: Waite Group Press, 1993.
15. Taylor RP. Fractal expressionism—where art meets science. In: Casti J, Karlqvist A, editors. Art and complexity. Amsterdam, The Netherlands: Elsevier Press, 2003;117–45.
16. Taylor RP, Spehar B, Wise JA, Clifford CWG, Newell BR, Hagerhall CM, et al. Perceptual and physiological responses to the visual complexity of Pollock's dripped fractal patterns. Nonlinear Dynamics Psychol Life Sci 2005;9(1):115–33.
17. Bevel T, Gardner RM. Bloodstain pattern analysis, 2nd edn. Boca Raton, FL: CRC Press, 2002.
18. MacDonnel HL. Bloodstain pattern interpretation. Corning, NY: Laboratory of Forensic Science, 1982.
19. Sandu AL, Rasmussen IA, Lundervold A, Kreuder F, Neckelmann G, Hugdahl K, et al. Fractal dimension analysis of MR images reveals grey matter structure irregularities in schizophrenia. Comput Med Imaging Graph 2008;32:150–8.
20. Smith TG, Lange GD, Marks WB. Fractal methods and results in cellular morphology dimensions, lacunarity and multifractals. J Neurosci Methods 1996;69:123–36.
21. Plotnick RE, Gardner RH, O'Neill RV. Lacunarity indices as measures of landscape texture. Landscape Ecol 1993;8(3):201–11.
22. Tang D, Marangoni AG. 3D fractal dimension of fat crystal networks. Chem Phys Lett 2006;433:248–52.
23. Ahammer H, DeVaney TTJ. The influence of edge detection algorithms of edge detection algorithm on the estimation of the fractal dimension of binary digital images. Chaos 2004;14(1):183–8.
24. Zhang L, Dean D, Liu JZ, Sahgal V, Wang X, Yue GH. Quantifying degeneration of white matter in normal aging using fractal dimension. Neurobiol Aging 2007;28:1543–55.

Additional information and reprint requests:
Scott I. Fairgrieve, Ph.D.
Department of Forensic Science
Laurentian University
935 Ramsey Lake Road
Sudbury
ON P3E 2C6
Canada
E-mail: sfairgrieve@laurentian.ca